Quantifying Riverbed Scour and Hydrodynamic Changes Induced by Bridge Piers in a Diurnal Tidal Estuary: A Pre-Construction Assessment of May Chai Bridge, Hai Phong City

Quan Tran-ANH[1)]; Ngoc Nguyen-Thi-HONG[2)*]
[1)] 1Faculty of Environment, University of Mining and Geology, Hanoi City, Vietnam
[2)] Faculty of Natural Resources and Environment, Vietnam National University of Agriculture, Vietnam

*Corresponding author: hongngockhtn@gmail.com

doi: 10.29227/IM-2026-01-01-019

ABSTRACT

Bridge construction in tidal estuaries poses significant risks to structural stability through pier-induced scour, yet comprehensive pre-construction assessments remain rare in Southeast Asia's dynamic river systems. This study quantified projected hydrodynamic and morphological impacts of the planned Mai Chai Bridge on Vietnam's Cam River using high-resolution MIKE 3 FM simulations before construction commenced. The model, calibrated against 2021–2022 field measurements (NSE = 0.92 for water levels, 0.56–0.67 for waves, 0.62–0.73 for sediment transport), revealed dramatic seasonal contrasts in pier impacts. During flood season, piers reduced upstream velocities by up to 80% (from 0.9 m/s to 0.1–0.2 m/s), generating complex turbulent wake patterns that extended 500–550 m downstream before flow recovery. Maximum seasonal scour depths of 0.4–0.5 m were projected adjacent to pier foundations, with pronounced asymmetric erosion along the left bank driven by channel curvature and secondary circulation. In contrast, dry season bidirectional tidal flows produced near-equilibrium conditions with minimal net morphological change (±0.05 m/season). These findings demonstrate that cumulative flood season scour dominates long-term foundation stability despite dry season recovery, with critical implications for pier embedment design, differential scour protection strategies, and adaptive maintenance protocols. This pre-construction modeling approach provides a cost-effective framework for predictive infrastructure assessment in monsoon-influenced tidal rivers worldwide.

KEYWORDS: b*ridge pier scour; 3D hydrodynamic modeling; sediment transport; MIKE 3 FM; morphodynamic processes*

1 INTRODUCTION

Bridge piers constitute essential but potentially disruptive elements in riverine and estuarine systems. By constricting flow cross-sections, piers alter conveyance capacity, elevate upstream water levels, and accelerate flows through contracted reaches (Wang et al., 2019; Setyandito et al., 2020). These hydraulic alterations generate complex three-dimensional flow patterns—including horseshoe vortices, wake turbulence, and flow acceleration—that intensify erosive forces on riverbeds and banks (Kummu et al., 2005; Islam et al., 2013). The resulting scour threatens structural integrity by undermining pier foundations and abutments, compromising bridge longevity and safety (Wang et al., 2019; McCartney, 2009).

These challenges intensify in tidal estuaries, where bidirectional flows, fluctuating water levels, and variable sediment transport create highly dynamic conditions (Uncles, 2003; Dalrymple et al., 1992; Dyer, 1997). Bridge construction in such environments can disrupt the delicate balance between riverine and marine forcing, altering tidal propagation, current patterns, and morphological evolution (Prandle, 2009; Gao et al., 2018). Field studies have documented intense turbulence and elevated bed shear stresses at bridge piers in tidal waterways (Ettema et al., 2011), with maximum scour depths often occurring during ebb tides when tidal and fluvial flows oppose each other (Umbrell et al., 1998). Laboratory investigations have further revealed that flow reversals exacerbate scour development, though pier geometry can mitigate erosion (Bearman et al., 2020; Umeda et al., 2003).

Numerical modeling, particularly three-dimensional computational fluid dynamics (CFD), has emerged as a powerful tool for quantifying pier-induced impacts. Gao et al. (2018) demonstrated significant alterations in flow and sediment patterns around bridge piers in the Yellow River estuary, while Zhao et al. (2015) emphasized the importance of coupled hydrodynamic-sediment transport models for accurate scour prediction in the Yangtze River estuary. Despite these advances, comprehensive studies quantifying combined hydrodynamic and morphological impacts in diurnal tidal estuaries remain limited, particularly in Southeast Asia.

Vietnam's extensive coastline and numerous tidal river systems present unique infrastructure challenges, exacerbated by climate change impacts including sea-level rise and intensified extreme events (Tran Anh & Taniguchi, 2014; Tran-Anh et al., 2023). Recent bridge failures and stability threats have been attributed to unanticipated morphological shifts and discharge fluctuations during monsoons (McCartney, 2009; Islam et al., 2013). While Nguyen et al. (2016) investigated local scour at bridge piers in the Thi Vai River estuary using physical modeling, and Tran et al. (2018) examined hydrodynamic impacts on the Hau River using 2D simulations, comprehensive 3D assessments of pier impacts in Vietnam's diurnal tidal estuaries remain scarce.

The planned May Chai Bridge will span the downstream section of the Cam River near Hai Phong City, approximately 30 km upstream from the Gulf of Tonkin. This site experiences a diurnal tidal regime with pronounced seasonal flow variations driven by monsoons. To address the research gap in pre-construction impact assessment, this study employs MIKE 3 FM—a sophisticated 3D hydrodynamic model developed by DHI (2017)—to simulate hydraulic conditions with and without the proposed bridge piers. By quantifying projected changes in water levels, velocities, and scour potential before construction, this research provides critical insights for scour mitigation strategies and resilient bridge design adapted to the Cam River's unique hydrodynamic regime.

2 DATA AND METHOD

2.1 Study area

The May Chai Bridge site is located on the Cam River, approximately 15 km southwest of Hai Phong city center and 30 km upstream from the Gulf of Tonkin (Fig. 1a). This reach experiences diurnal tidal influence with a single high-low tide cycle daily. The river channel at the bridge location is 60–80 m wide, draining a catchment area of approximately 250 km². The riverbed comprises alluvial deposits dominated by sand and gravel, with an average longitudinal slope of 0.001.

The flow regime exhibits strong seasonality with high flows occur during the flood season (May–October) driven by monsoonal rainfall, while low flows characterize the dry season (December–April). The proposed bridge consists of three spans totaling 180 m in length with an 18-m-wide deck (Fig. 2a). Two circular reinforced concrete piers (2 m diameter) will support the structure, each founded on 32 piles (Fig. 2b). The bridge alignment crosses the river at approximately 45°.

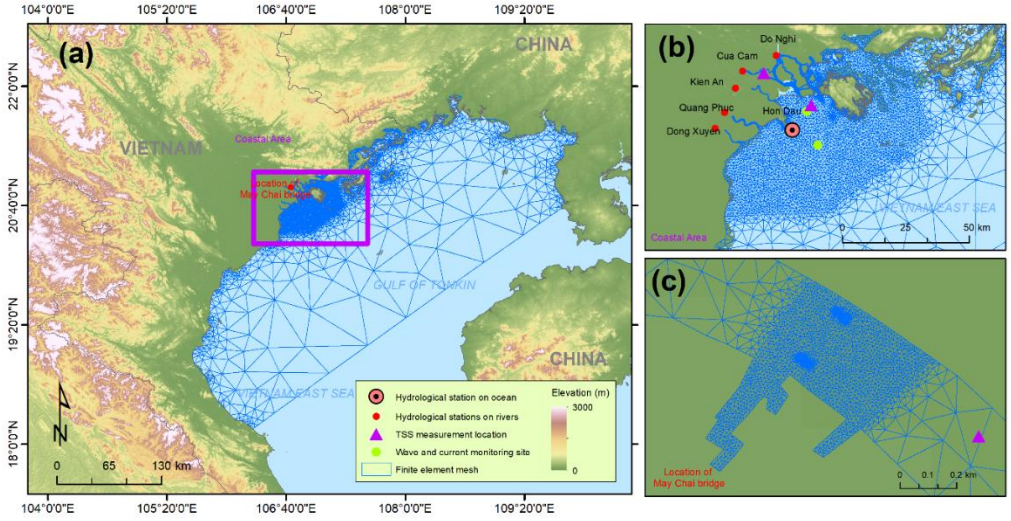

Figure 1. Overview of the study area and model setup, showing (a) the relative location of the May Chai Bridge and the Gulf of Tonkin with the finite-element mesh, (b) upstream boundaries and hydrological and TSS observation sites, and (c) the high-resolution finite-element mesh around the bridge pier foundations.

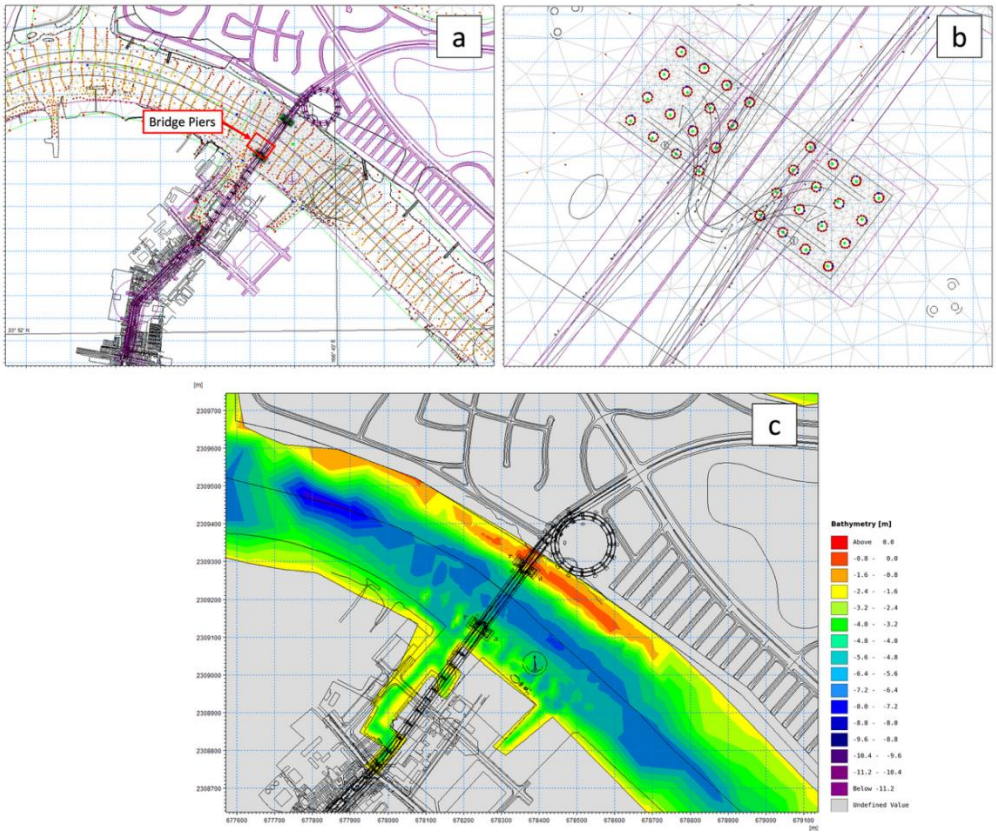

Figure 2. Engineering and geomorphic characteristics of the May Chai Bridge site, illustrating (a) the overall bridge layout, (b) the detailed design and arrangement of the 32 bridge piers at their foundations, and (c) the riverbed bathymetry of the study area.

2.2 Numerical Modeling Framework

2.2.1 MIKE 3 FM Hydrodynamic Model

MIKE 3 FM solves the three-dimensional incompressible Reynolds-averaged Navier-Stokes equations on a flexible mesh, simulating complex flows and water level variations in rivers, estuaries, and coastal waters (DHI, 2017). The model accounts for bathymetry, bed roughness, turbulence closure, and hydraulic structures. The dynamic coupling between flow, water levels, and structures renders MIKE 3 FM well-suited for evaluating localized pier impacts (Islam et al., 2014; Roul et al., 2022).

2.2.2 Sediment Transport Module

The Mud Transport (MT) module simulates erosion, transport, and deposition of cohesive and non-cohesive sediments, incorporating bed load transport, suspended load dynamics, and bed-water column exchange processes (DHI, 2017). This module enables quantification of temporal morphological changes induced by scour.

2.3 Model Configuration

2.3.1 Computational Domain and Mesh

To adequately represent the complex hydraulic conditions influenced by multiple rivers in the Red River system, the computational domain extends from Hainan Island, China, to Ha Tinh Province, Vietnam, covering 850 km of coastline and extending 180 km offshore (Fig. 1a). The finite element mesh employs coarse resolution offshore with progressive refinement toward the coast and river mouths. An ultra-high-resolution mesh surrounds the bridge site to resolve micro-scale hydrodynamic changes induced by the piers (Fig. 1b,c).

2.3.2 2.3.2. Boundary Conditions

The model incorporates one offshore boundary and five upstream river boundaries (Fig. 1b). Offshore water levels were prescribed using the MIKE 21 Global Tidal Model (Carrere et al., 2012), which incorporates tidal constituents to accurately represent tidal dynamics. Upstream river boundaries utilized discharge data from five hydrological stations: Dong Xuyen (Thai Binh River), Quang Phuc (Van Uc River), Kien An (Lach Tray River), Cua Cam (Cam River), and Do Nghi (Bach Dang River).

Wave conditions were simulated using the MIKE 21 Spectral Wave (SW) model, forced by offshore wind data to account for wind-driven wave influences on coastal and estuarine hydrodynamics.

2.4 Input Data

2.4.1 Hydrometeorological Data

River discharge data (2021–2022) were obtained from Vietnam's National Center for Hydro-Meteorological and Environmental Forecasting. Wind data were extracted from the European Centre for Medium-Range Weather Forecasts (ECMWF) ERA5 global reanalysis (Hersbach et al., 2020), providing hourly wind fields at 10 km spatial resolution. Data were specifically extracted for the Southwest monsoon (June–August, flood season) and Northeast monsoon (December–February, dry season).

Acoustic Wave and Current profilers (AWACs) deployed at offshore and nearshore locations continuously measured current velocity, wave height, peak period, and wave direction. Multiple deployment campaigns spanning June 2021 to May 2022 captured seasonal and extreme conditions, with individual campaigns lasting 15 days to 3 months.

Water samples for total suspended solids (TSS) analysis were collected at two locations (downstream of the bridge site and adjacent coastal waters) over 16 days (July 13–28, 2021) (Fig. 1b). Hourly water level data from Hon Dau station (2021–2022) captured tidal, storm surge, and seasonal variations. Offshore wave boundary conditions were validated against NCEP/NOAA WAVEWATCH III model outputs.

2.4.2 Topographic and Bathymetric Data

Bathymetric data were compiled from multiple sources: GEBCO global data (15 arc-second resolution) for deep offshore regions (Mayer et al., 2018), regional bathymetry (1:250,000 scale) from Vietnam's Ministry of Natural Resources and Environment (MONRE)

for nearshore transitions, high-resolution surveys (1:50,000 scale) conducted in 2017 along the Hai Phong coast, and supplemental multibeam echosounder surveys within the Cam estuary to capture topographic features around the planned bridge location (Fig. 2c).

2.4.3 Sediment Characteristics

Five bottom sediment samples collected on July 15, 2022, were analyzed for particle size distribution (Table 1). Average composition comprised 11.3% coarse sand (0.2–2 mm), 31.6% fine sand (0.02–0.2 mm), 48.1% silt (0.002–0.02 mm), and 8.9% clay (<0.002 mm). The dominance of silt reflects the overall sediment character, while sand presence indicates energetic transport capacity during high flows.

Table 1. Analysis of grain size percentages in sediment samples collected from the Cam River channel

Sample No.	Composition of sediment (%)			
	Coarse sand (2–0.2 mm)	Fine sand (0.2–0.02 mm)	Mud (0.02–0.002 mm)	Silt (<0.002 mm)
1	11.85	37.48	45.28	5.39
2	9.48	31.48	43.28	15.76
3	11.48	28.49	50.42	9.61
4	13.32	28.49	48.59	9.6
5	10.48	32.18	53.12	4.22

2.5 Initial Conditions

Hydrodynamic and wave models were initialized with zero water levels, velocities, and wave parameters, allowing natural pattern development from forcing. The sediment model employed uniform initial TSS concentrations based on average measured values, permitting evolution through model spin-up.

2.6 Model Calibration and Validation

Model performance was assessed using the Nash-Sutcliffe Efficiency (NSE) index (Nash and Sutcliffe, 1970; Krause et al., 2005). Calibration involved adjusting parameters including bed roughness (0.005), turbulent viscosity coefficient (0.28), convergence coefficient (0.80), wave breaking coefficient (0.76), horizontal diffusivity coefficient (1.00), sediment internal friction angle (30°), and bed friction coefficient (0.001) (Table 2).

Table 2. Key model parameters utilized for simulation

TT	Model parameters	Value
1	Bed roughness	0.005
2	Turbulent viscosity coefficient	0.28
3	Convergence coefficient	0.80
4	Wave breaking coefficient	0.76
5	Horizontal diffusivity coefficient	1.00

TT	Model parameters	Value
6	Internal friction angle of sediment	30°
7	Bed friction coefficient	0.001

3 RESULTS AND DISCUSSION

3.1 Model Verification and Calibration

3.1.1 Water Level and Wave Dynamics

Water level calibration at Hon Dau station achieved NSE = 0.92 (Fig. 3), demonstrating excellent model skill in replicating tidal dynamics. This provides a robust foundation for simulating interconnected coastal and estuarine processes.

Wave model validation yielded NSE values of 0.67 for wave velocity, 0.62 for wave direction, and 0.56 for significant wave height (Fig. 4a–c). While the model slightly underestimated peak wave velocities and overestimated minimum speeds, overall performance was satisfactory given the complex bathymetry and coastal geometry of the Gulf of Tonkin (Piton, 2019). These results confirm the model's capability to represent regional wave transformation processes.

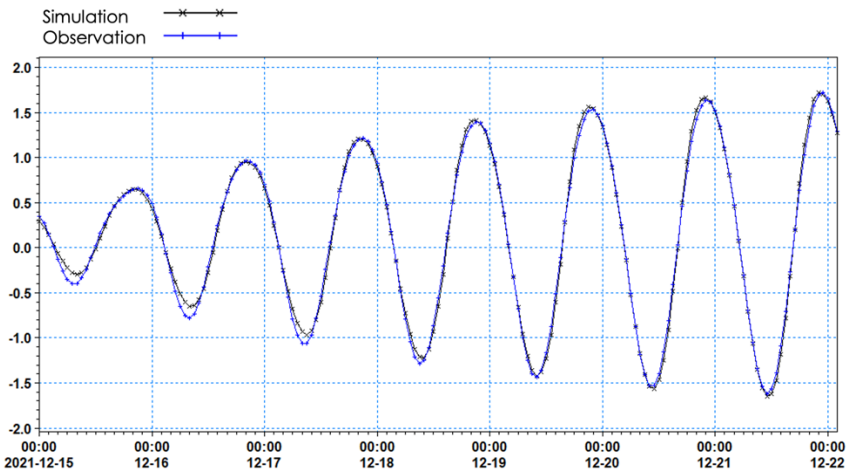

Figure 3. Comparison of the simulated and measured water level at Hon Dau station

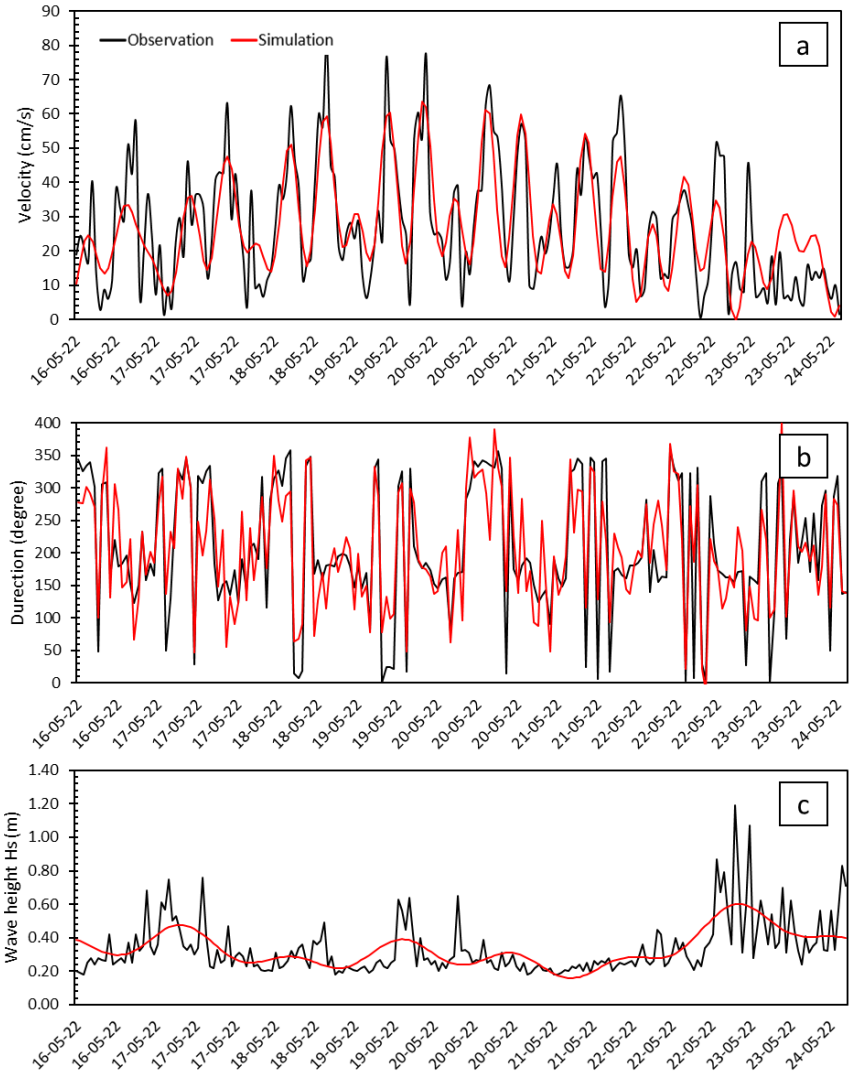

Figure 4. Comparison of the simulated and measured (a) wave velocity, (b) wave direction, and (c) wave height at the projection site

3.1.2 Sediment Transport Validation

TSS simulations achieved NSE values of 0.73 for the coastal region and 0.62 for the bridge area (Fig. 5). Performance was superior in deeper coastal waters compared to the shallower bridge reach, where cross-sectional heterogeneity increases due to bed-flow interactions. The moderate NSE values align with performance reported in similar coastal and estuarine studies (Ralston et al., 2013; Warner et al., 2005; Tran-Anh et al., 2022), acknowledging the inherent challenges of modeling fine sediment dynamics during high-flow events when enhanced resuspension, advection, and deposition occur (Geleynse et al., 2011; Bouillon et al., 2007; Bi et al., 2014).

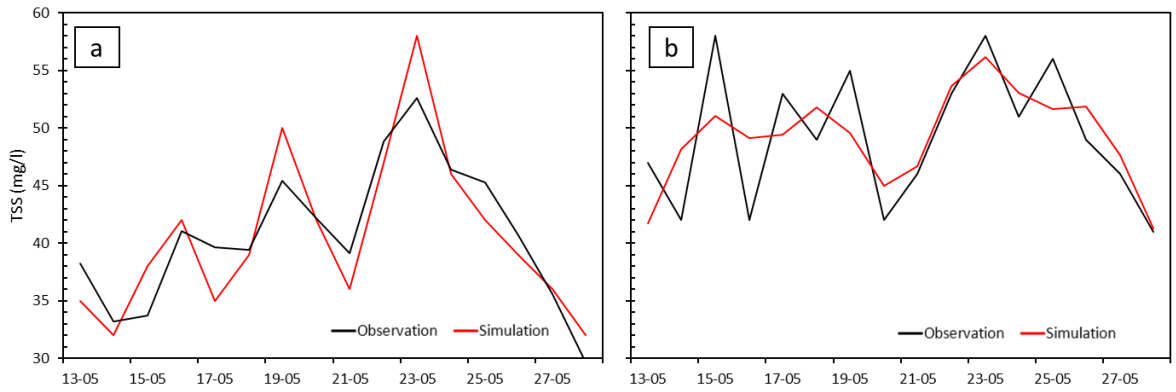

Figure 5. Measured and simulated TSS concentration in the project area for (a) the coastal region and (b) the May Chai bridge area

3.2 Bridge Pier Impacts on Flow Dynamics

3.2.1 Flood Season Hydraulics

During flood season, high monsoonal discharge dominates the flow regime despite diurnal tidal influence (Fig. 6). Without bridge piers, average velocities at the bridge location exceed 0.9 m/s, with higher velocities along the left (seaward) bank due to channel curvature. Pier installation significantly reduces upstream velocities to 0.1–0.2 m/s as the structures obstruct and dampen flow. This velocity reduction extends along both banks, while mid-channel velocities increase slightly to maintain discharge continuity. Approximately 500–550 m downstream, flow patterns gradually recover to pre-construction conditions, indicating localized pier influence during flood season.

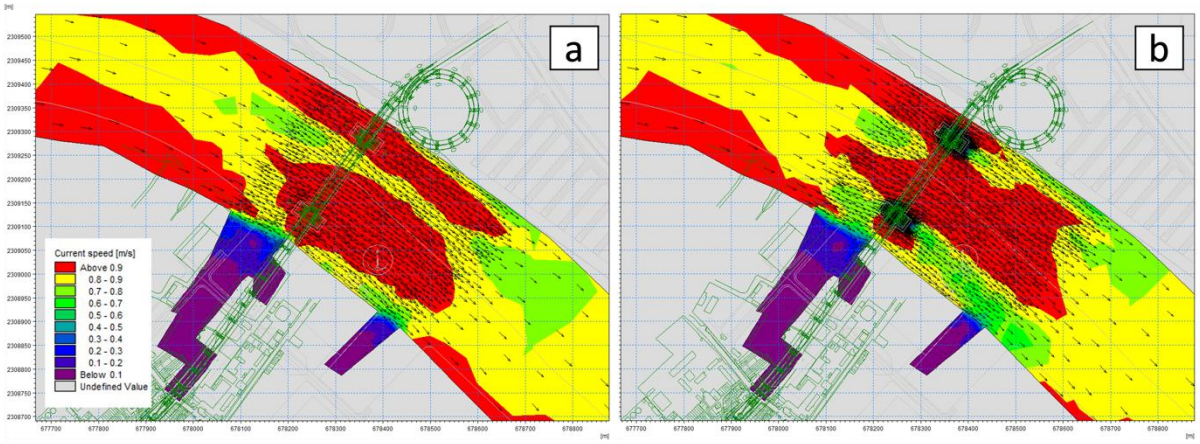

Figure 6. Seasonally averaged flow patterns of the Cam River during flood season in 2022 at high tide phase: (a) before and (b) after the construction of May Chai Bridge. Arrows indicate the directions of water flow

3.2.2 Dry Season Hydraulics

The dry season exhibits lower discharges and enhanced tidal influence, resulting in bidirectional flow (Fig. 7). During high tide, outflow persists but weakens compared to flood

season. During low tide, tidal inflow progressively replaces upstream discharge until flow reverses landward. Flow velocities at pier locations range from 0.3–0.4 m/s without piers, reducing to 0.2–0.3 m/s post-construction.

Complex turbulent patterns develop around the piers, particularly during tidal transitions (Fig. 8). Seaward flow slightly exceeds landward flow, evidenced by higher velocities during ebb tide. Proximity to the riverbed enhances turbulence around piers relative to open channel areas. During tidal flow reversals, intensified flows develop in pier-free zones while localized velocity reductions occur near structures, creating distinct wake patterns that evolve with the tidal cycle.

These hydraulic alterations align with previous research. Velocity reductions of 35–40% around piers due to flow contraction are consistent with findings by Dey and Raikar (2007). Complex turbulent patterns near piers agree with observations by Kandasamy and Melville (1998) and Ettema et al. (2010). The sensitivity of pier hydraulic impacts to seasonal and tidal conditions reinforces findings by Tingsanchali and Maheswaran (1990), who emphasized that short-term measurements may not capture the full range of scour risk across hydrologic scenarios.

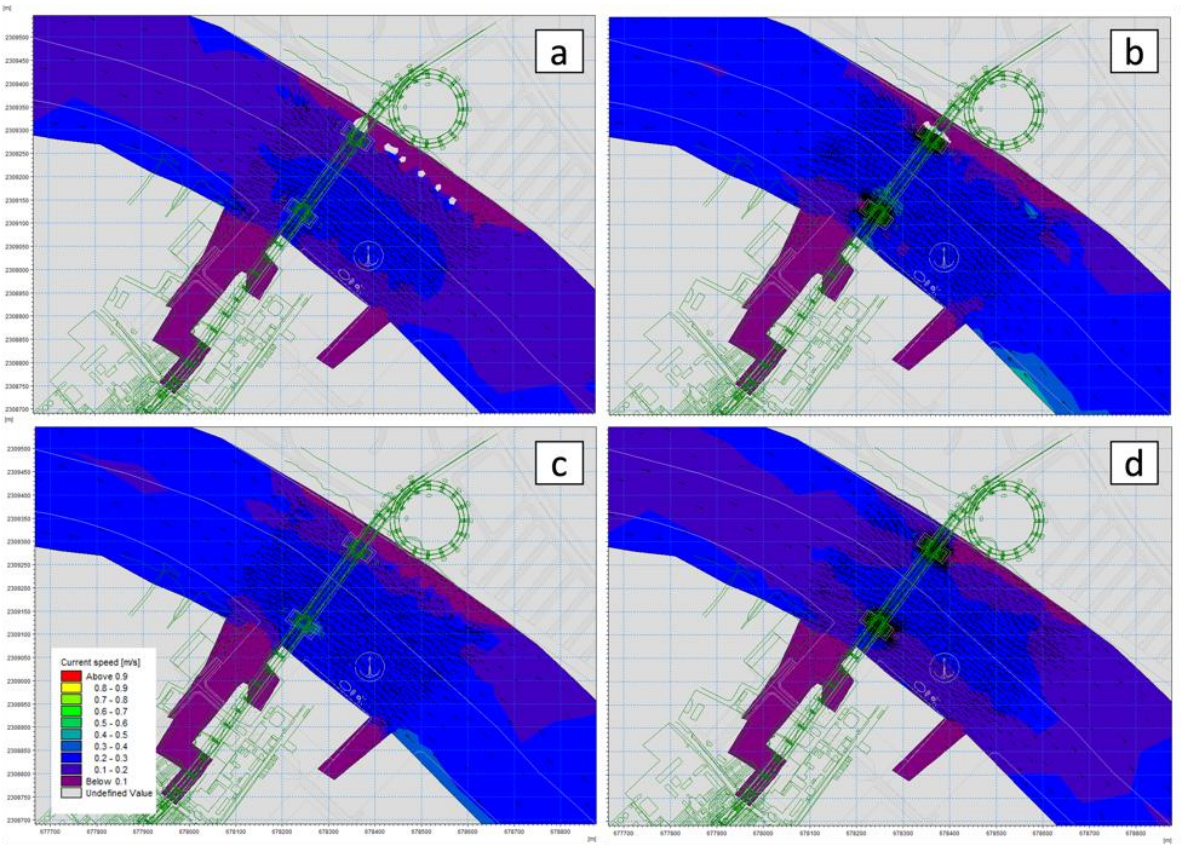

Figure 7. Flow patterns of the Cam River during dry seasons in low tide (a, b) and high tide (c, d) phases. The sequence from left to right represents the conditions after and before the construction of the May Chai bridge

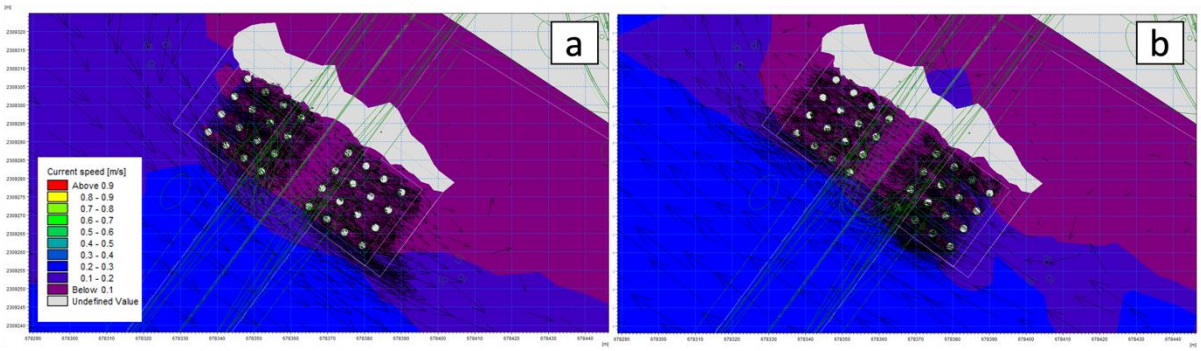

Figure 8. Flow dynamics in the May Chai left piers in dry season in (a) low tide and (b) high tide phases

3.3 Riverbed Scour Assessment

3.3.1 Flood Season Morphological Changes

Simulations under 2022 flood conditions reveal that meandering morphology renders this Cam River reach prone to natural scour, particularly near proposed pier foundations (Fig. 9). Natural bank erosion persists on meander bend exteriors (−0.3 to −0.5 m/season), while sedimentation occurs along inner bends (+0.1 to +0.2 m/season) due to topographic flow steering.

Bridge piers significantly amplify erosion and sedimentation patterns proximal to the infrastructure. Additional scour of −0.1 to −0.2 m develops both upstream and downstream of piers during floods, with more substantial erosion reaching −0.3 to −0.4 m/season along unprotected riverbed adjacent to pier foundations (Fig. 10). Within 20–25 m downstream, flow deceleration produces sedimentation rates of +0.2 to +0.5 m/season. This differential pattern reflects additional turbulence and flow constriction imposed by the piers. Channel sinuosity and associated secondary flows concentrate erosion along the left bank during floods, resulting in maximum seasonal scour depths of approximately 0.45 m at the left pier foundation.

These simulated values represent seasonal morphodynamic responses to sustained flood flows rather than instantaneous design scour depths, which would require event-based modeling of extreme discharge scenarios. The predicted seasonal scour provides critical insights for long-term foundation monitoring and maintenance planning.

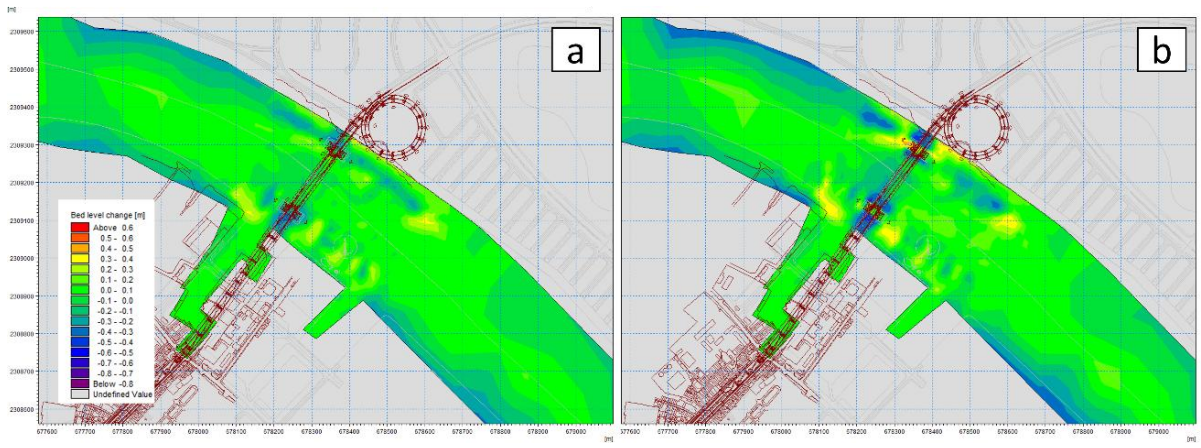

Figure 9. Erosion within the Cam Riverbed during the flood season, both before (a) and after (b) the construction of the May Chai Bridge

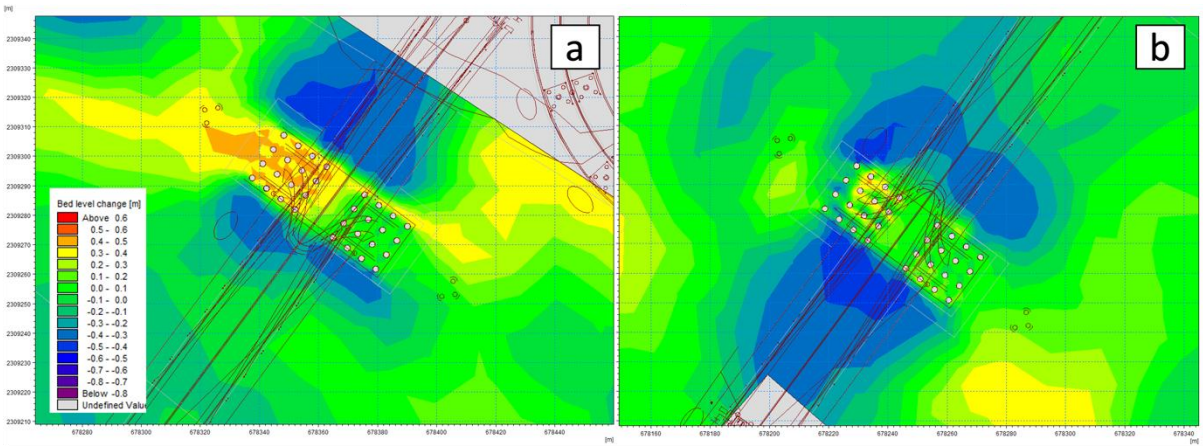

Figure 10. Morphological characteristics of river bed during the flood season at the (a) left and (b) right piers

3.3.2 Dry Season Morphological Changes

During dry season, reduced discharge and bidirectional tidal flows produce muted morphological changes. Topographic variations fluctuate within ±0.05 m/season around the bridge, approaching morphodynamic equilibrium. Slight net sedimentation dominates, averaging 0.01–0.015 m/season across the riverbed and increasing to 0.01–0.02 m/season adjacent to piers. This sedimentation dominance demonstrates greater stability under dry season conditions relative to scour-prone monsoonal floods.

The pronounced flood season scour aligns with field measurements by Ettema et al. (2010), demonstrating correlations between scour depth and flow intensity. The relatively moderate erosion magnitudes (compared to sandy substrates) reflect cohesive, fine-grained bed composition, as discussed by Briaud et al. (2011) regarding scour reduction in clay-rich versus sandy substrates. The cohesive sediment constrains erosion pit formation, partially mitigating impacts on pier base stability—a critical consideration for long-term bridge safety. Since flood season scour dominates over dry season sedimentation, cumulative seasonal cycles favor net erosion around pier foundations. Although dry season erosion magnitude is lower, pier wake turbulence produces localized scour with potential to threaten structural integrity through progressive undermining and abrasion over multiple monsoon cycles.

3.4 Engineering Implications

The quantified hydrodynamic alterations and morphological responses provide essential information for bridge design and scour countermeasures. Maximum seasonal scour depths of 0.4–0.5 m adjacent to pier foundations indicate that pier embedment depth must exceed these values with appropriate safety factors. Asymmetric erosion patterns favoring the left bank suggest that differential scour protection may be more cost-effective than uniform protection schemes. The recovery of flow patterns 500–550 m downstream indicates localized pier influence, suggesting that ecological impacts on fish migration and sediment transport may be spatially limited. However, the complex turbulent wake patterns during dry season tidal reversals warrant monitoring for potential impacts on benthic habitats and sediment oxygen demand.

The demonstrated capability of 3D numerical modeling for pre-construction assessment provides a cost-effective complement to physical modeling. For the May Chai Bridge, these results will inform selection of appropriate scour protection (e.g., riprap sizing and extent), foundation monitoring protocols, and adaptive maintenance strategies tailored to seasonal flow variations.

4 CONCLUSIONS

This pre-construction assessment of the Mai Chai Bridge demonstrates how advanced 3D hydrodynamic modeling can quantify infrastructure impacts before construction, providing critical insights for resilient design in dynamic tidal rivers. Validated against 2021–2022 field observations (NSE = 0.62–0.92 across water levels, waves, and sediment transport), the MIKE 3 FM simulations revealed stark seasonal contrasts in pier-induced hydraulic alterations and scour potential.

The comparative simulations revealed the dominance of flood season processes in controlling long-term morphological evolution. Bridge piers will reduce upstream velocities by up to 80% (0.9 m/s to 0.1–0.2 m/s) during monsoons, generating complex turbulent wakes that drive maximum seasonal scour depths of 0.4–0.5 m adjacent to foundations. Asymmetric erosion patterns, with pronounced left-bank scour driven by channel curvature and secondary circulation, indicate that uniform scour protection would be inefficient and costly. In contrast, dry season bidirectional tidal flows approach morphodynamic equilibrium, permitting modest sediment recovery but insufficient to offset cumulative flood season erosion over multiple monsoon cycles.

These findings carry direct engineering implications. Pier embedment depths for this region must exceed 0.5 m with appropriate safety factors, while differential scour protection targeting the left bank offers a cost-effective alternative to uniform countermeasures. The localized spatial extent of pier influence (flow recovery within 500–550 m downstream) suggests limited ecological disruption to fish migration corridors and regional sediment transport, though site-specific monitoring during construction is recommended.

Beyond the Mai Chai Bridge, this study establishes a transferable methodology for pre-construction impact assessment in monsoon-influenced tidal estuaries worldwide. As climate change intensifies extreme rainfall and alters seasonal flow regimes across Southeast Asia, predictive 3D modeling becomes increasingly essential for infrastructure planning that balances development needs with morphological stability and environmental sustainability. The quantified seasonal scour dynamics presented here provide a foundation for adaptive management strategies that can respond to evolving hydroclimatic conditions throughout bridge operational lifespans.

Conflict of Interest Statement

The authors declare that they have no known competing financial interests or personal relationships that could have appeared to influence the work reported in this paper. This research was conducted independently and objectively, and the analyses, interpretations, and conclusions presented are based solely on scientific considerations. No commercial, institutional, or contractual interests influenced the study design, data analysis, or reporting of results.

Author Contributions

Q.T.A was responsible for study conception, numerical model development, simulation design, and primary data analysis. N.N.T.H contributed to data acquisition, model calibration and validation, and supported result interpretation. Both authors jointly drafted, revised, and approved the final manuscript.

5 REFERENCES

[1] Bearman, P.W., Kemmelmeier, J., & Xie, Z. (2020). Effects of tidal flow reversals on scour around bridge piers. Journal of Hydraulic Engineering, 146(7), 04020037.

[2] Bi, Q., Toorman, E.A., Smits, J., Wang, Y., & Wang, X. (2014). Modeling sediment transport in the Yellow River Estuary: Challenges and considerations. Coastal Engineering, 87, 57–69.

[3] Bouillon, S., Frankignoulle, M., Dehairs, F., Velimirov, B., Eiler, A., Abril, G., Etcheber, H., & Borges, A.V. (2007). Contrasting biogeochemical characteristics of the Orinoco River and the Guadalquivir Estuary in the deposition zone of the tropical Atlantic Ocean. Journal of Geophysical Research: Oceans, 112(C12).

[4] Briaud, J.L., Chen, H.C., Chang, K.A., Oh, S.J., Chen, S., Chen Wang, J., Li, Y., Kwak, K., Nartjaho, P., Gudaralli, R., Wei, W., Pergu, S., Cao, Y.W., & Ting, F. (2011). The Sricos-EFA method. Summary Report, Texas A&M University, College Station, TX.

[5] Carrere, L., Lyard, F., Cancet, M., Guillot, A., & Roblou, L. (2012). FES 2012: A new global tidal model taking advantage of nearly 20 years of altimetry. In 20 Years of Progress in Radar Altimetry, 710, 13.

[6] Dalrymple, R.W., Zaitlin, B.A., & Boyd, R. (1992). Estuarine facies models: Conceptual basis and stratigraphic implications. Journal of Sedimentary Research, 62(6), 1130–1146.

[7] Dey, S., & Raikar, R.V. (2007). Characteristics of horseshoe vortex in developing scour holes at piers. Journal of Hydraulic Engineering, 133(4), 399–413.

[8] DHI (2017). MIKE Powered by DHI. [Online] Available at: https://www.mikepoweredbydhi.com/products/mike-3-wave-fm [Accessed 15 March 2023].

[9] Dyer, K.R. (1997). Estuaries: A Physical Introduction. John Wiley & Sons Ltd.

[10] Ettema, R., Melville, B.W., & Barkdoll, B. (2011). Scale effects in pier-scour experiments. Journal of Hydraulic Engineering, 137(10), 1203–1217.

[11] Ettema, R., Nakato, T., & Muste, M. (2010). Estimation of scour depth at bridge abutments. NCHRP Report 24-20, Transportation Research Board, Washington D.C.

[12] Gao, J., Gao, S., Fang, H., & Wang, Y. (2018). Numerical study on the hydrodynamic effects of bridge piers on the transport of suspended sediment in the Yellow River. Ocean Engineering, 164, 110–122.

[13] Geleynse, N., Storms, J.E.A., Walstra, D.I.R., Jagers, H.R.A., Wang, Z.B., & Stive, M.J.F. (2011). Controls on river-plume sediment dispersal. Water Resources Research, 47(6).

[14] Hersbach, H., Bell, B., Berrisford, P., Hirahara, S., Horányi, A., Muñoz-Sabater, J., Nicolas, J., Peubey, C., Radu, R., Schepers, D., Simmons, A., Soci, C., Abdalla, S., Abellan, X., Balsamo, G., Bechtold, P., Biavati, G., Bidlot, J., Bonavita, M., ... Thépaut, J. (2020). The ERA5 global reanalysis. Quarterly Journal of the Royal Meteorological Society, 146(730), 1999–2049. https://doi.org/10.1002/qj.3803

[15] Islam, A.S., Haque, A., & Islam, G.M.T. (2013). Necessity of monitoring for bridge pier scour in Bangladesh. Geomechanics and Engineering, 5(5), 425–438.

[16] Islam, M.R., Zhu, D.Z., & Rahman, M.M. (2014). Monitoring hydraulic performance of bridge and evaluating scour depth using data-driven models based on cluster and classification analyses. Journal of Computing in Civil Engineering, 29(6), 04014075. https://doi.org/10.1061/(ASCE)CP.1943-5487.0000416

[17] Kandasamy, J.K., & Melville, B.W. (1998). Maximum local scour depth at bridge abutments. Journal of Hydraulic Research, 36(2), 183–201.

[18] Krause, P., Boyle, D.P., & Basee, F. (2005). Comparison of different efficiency criteria for hydrological model assessment. Advances in Geosciences, 5, 89–97.

[19] Kummu, M., Koponen, J., & Sarkkula, J. (2005). Assessing impacts of the Mekong development in the Tonle Sap Lake. In Modelling and Management of Sustainable Basin-scale Water Resource Systems (pp. 157–182). IAHS Publ.

[20] Mayer, L., Jakobsson, M., Allen, G., Dorschel, B., Falconer, R., Ferrini, V., ... & Weatherall, P. (2018). The Nippon Foundation–GEBCO seabed 2030 project: The quest to see the world's oceans completely mapped by 2030. Geosciences, 8(2), 63.

[21] McCartney, M. (2009). Living with dams: Managing the environmental impacts. Water Policy, 11(S1), 121–139.

[22] Nash, J.E., & Sutcliffe, J.V. (1970). River flow forecasting through conceptual models part I—A discussion of principles. Journal of Hydrology, 10(3), 282–290.

[23] Nguyen, T.H., Le, T.V., & Pham, V.N. (2016). Local scour around bridge piers in the Thi Vai River estuary, Vietnam. Journal of Coastal Research, 32(4), 867–875.

[24] Piton, V. (2019). From the Red River to the Gulf of Tonkin: Dynamics and Sediment Transport along the Estuary-Coastal Area Continuum. Doctoral dissertation, Université Paul Sabatier-Toulouse III.

[25] Prandle, D. (2009). Estuaries: Dynamics, Mixing, Sedimentation and Morphology. Cambridge University Press.

[26] Ralston, D.K., Geyer, W.R., & Warner, J.C. (2013). Sediment transport due to extreme events: The Hudson River estuary after tropical storms Irene and Lee. Geophysical Research Letters, 40(20), 5451–5455.

[27] Roul, A.K., Ghoshal, K., & Mazumder, B.S. (2022). Modeling flow field around hydraulically complex pier with debris accumulation in post-monsoon season. Applied Water Science, 12(3). https://doi.org/10.1007/s13201-022-01587-7

[28] Setyandito, O., Alexander Michael, R.D., Juliastuti, Andrew, J.P., & Wijayanti, Y. (2020). The effect of bridge abutment shape variation toward flow velocity characteristic. IOP Conference Series: Earth and Environmental Science, 426(1), 012035. https://doi.org/10.1088/1755-1315/426/1/012035

[29] Tingsanchali, T., & Maheswaran, S. (1990). 2-D depth-averaged flow computation near bridge abutments. Journal of Hydraulic Engineering, 116(1), 71–86.

[30] Tran Anh, Q., & Taniguchi, K. (2014). Variations of precipitation and water resources in the northern part of Vietnam under climate change. Journal of Japan Society of Civil Engineers, Ser. B1 (Hydraulic Engineering), 70(4), I_211–I_216. https://doi.org/10.2208/jscejhe.70.I_211

[31] Tran-Anh, Q., Ngo-Duc, T., Espagne, E., & Trinh-Tuan, L. (2023). A 10-km CMIP6 downscaled dataset of temperature and precipitation for historical and future Vietnam climate. Scientific Data, 10(1), 257. https://doi.org/10.1038/s41597-023-02159-2

[32] Tran-Anh, Q., Tanaka, H., & Duy, D.V. (2022). Modeling suspended sediment dynamics in the Mekong Delta under changing environmental conditions. Coastal Engineering Journal, 64(2), 245–262.

[33] Tran, V.L., Nguyen, T.A., & Le, H.M. (2018). Hydrodynamic impacts of bridge construction on the Hau River, Vietnam. Journal of Hydro-environment Research, 20, 43–55.

[34] Umbrell, E.R., Lohnes, R.A., & Spencer, P.M. (1998). Local scour at bridge piers in tidal waterways. Journal of Hydraulic Engineering, 124(10), 1051–1057.

[35] Umeda, S., Ishida, H., & Yamazaki, M. (2003). Effects of pier shape on local scour around bridge piers. Water Science and Technology, 47(6–7), 235–242.

[36] Uncles, R.J. (2003). From catchment to coastal zone: Examples of the application of models to some long-term problems. Science of the Total Environment, 314, 567–594.

[37] Wang, W., Zhou, K., Jing, H., Zuo, J., Li, P., & Li, Z. (2019). Effects of bridge piers on flood hazards: A case study on the Jialing River in China. Water, 11(6), 1181. https://doi.org/10.3390/w11061181

[38] Warner, J.C., Geyer, W.R., & Lerczak, J.A. (2005). Numerical modeling of an estuary: A comprehensive skill assessment. Journal of Geophysical Research: Oceans, 110(C5).

[39] Zhao, M., Zhu, X., Vaziri, N., & Simon, B. (2015). A numerical investigation of local scour around bridge piers in the Yangtze River Estuary, China. Environmental Fluid Mechanics, 15(3), 603–632.